Measurement of the W-Boson P_T Distribution in $\bar{p}p$ Collisions at $\sqrt{s}=1.8$ TeV

F. Abe,[9] D. Amidei,[4] G. Apollinari,[12] M. Atac,[4] P. Auchincloss,[14] A. R. Baden,[6] A. Bamberger,[4,a] B. A. Barnett,[8] A. Barbaro-Galtieri,[10] V. E. Barnes,[13] F. Bedeschi,[12] S. Behrends,[2] S. Belforte,[12] G. Bellettini,[12] J. Bellinger,[20] J. Bensinger,[2] A. Beretvas,[4] J. P. Berge,[4] S. Bertolucci,[5] S. Bhadra,[7] M. Binkley,[4] R. Blair,[1] C. Blocker,[2] V. Bolognesi,[12] A. W. Booth,[4] C. Boswell,[8] G. Brandenburg,[6] D. Brown,[6] E. Buckley,[16] H. S. Budd,[14] A. Byon,[13] K. L. Byrum,[20] C. Campagnari,[3] M. Campbell,[3] R. Carey,[6] W. Carithers,[10] D. Carlsmith,[20] J. T. Carroll,[4] R. Cashmore,[4,a] F. Cervelli,[12] K. Chadwick,[4] G. Chiarelli,[5] W. Chinowsky,[10] S. Cihangir,[4] A. G. Clark,[4] D. Connor,[11] M. Contreras,[2] J. Cooper,[4] M. Cordelli,[5] D. Crane,[4] M. Curatolo,[5] C. Day,[4] S. Dell'Agnello,[12] M. Dell'Orso,[12] L. Demortier,[2] P. F. Derwent,[3] T. Devlin,[16] D. DiBitonto,[17] R. B. Drucker,[10] J. E. Elias,[4] R. Ely,[10] S. Eno,[3] S. Errede,[7] B. Esposito,[5] B. Flaugher,[16] G. W. Foster,[4] M. Franklin,[6] J. Freeman,[4] H. Frisch,[3] Y. Fukui,[9] Y. Funayama,[18] A. F. Garfinkel,[13] A. Gauthier,[7] S. Geer,[6] P. Giannetti,[12] N. Giokaris,[15] P. Giromini,[5] L. Gladney,[11] M. Gold,[10] K. Goulianos,[15] H. Grassmann,[12] C. Grosso-Pilcher,[3] C. Haber,[10] S. R. Hahn,[4] R. Handler,[20] K. Hara,[18] R. M. Harris,[10] J. Hauser,[3] T. Hessing,[17] R. Hollebeek,[11] L. Holloway,[7] P. Hu,[16] B. Hubbard,[10] B. T. Huffman,[13] R. Hughes,[11] P. Hurst,[5] J. Huth,[4] M. Incagli,[12] T. Ino,[18] H. Iso,[18] H. Jensen,[4] C. P. Jessop,[6] R. P. Johnson,[4] U. Joshi,[4] R. W. Kadel,[10] T. Kamon,[17] S. Kanda,[18] D. A. Kardelis,[7] I. Karliner,[7] E. Kearns,[6] L. Keeble,[17] R. Kephart,[4] P. Kesten,[2] R. M. Keup,[7] H. Keutelian,[7] S. Kim,[18] L. Kirsch,[2] K. Kondo,[18] S. E. Kuhlmann,[1] E. Kuns,[16] A. T. Laasanen,[13] J. I. Lamoureux,[20] S. Leone,[12] W. Li,[1] T. M. Liss,[7] N. Lockyer,[11] C. B. Luchini,[7] P. Maas,[4] M. Mangano,[12] J. P. Marriner,[4] R. Markeloff,[20] L. A. Markosky,[20] R. Mattingly,[2] P. McIntyre,[17] A. Menzione,[12] T. Meyer,[17] S. Mikamo,[9] M. Miller,[3] T. Mimashi,[18] S. Miscetti,[5] M. Mishina,[9] S. Miyashita,[18] Y. Morita,[18] S. Moulding,[2] A. Mukherjee,[4] L. F. Nakae,[2] I. Nakano,[18] C. Nelson,[4] C. Newman-Holmes,[4] J. S. T. Ng,[6] M. Ninomiya,[18] L. Nodulman,[1] S. Ogawa,[18] R. Paoletti,[12] A. Para,[4] E. Pare,[6] J. Patrick,[4] T. J. Phillips,[6] R. Plunkett,[4] L. Pondrom,[20] J. Proudfoot,[1] G. Punzi,[12] D. Quarrie,[4] K. Ragan,[11] G. Redlinger,[3] J. Rhoades,[20] M. Roach,[19] F. Rimondi,[4,a] L. Ristori,[12] T. Rohaly,[11] A. Roodman,[3] W. K. Sakumoto,[14] A. Sansoni,[5] R. D. Sard,[7] A. Savoy-Navarro,[4] V. Scarpine,[7] P. Schlabach,[7] E. E. Schmidt,[4] M. H. Schub,[13] R. Schwitters,[6] A. Scribano,[12] S. Segler,[4] Y. Seiya,[18] M. Sekiguchi,[18] M. Shapiro,[10] M. Sheaff,[20] M. Shochet,[3] J. Siegrist,[10] P. Sinervo,[11] J. Skarha,[8] K. Sliwa,[19] D. A. Smith,[12] F. D. Snider,[8] L. Song,[11] R. St. Denis,[6] A. Stefanini,[12] G. Sullivan,[3] R. L. Swartz, Jr.,[7] M. Takano,[18] F. Tartarelli,[12] K. Takikawa,[18] S. Tarem,[2] D. Theriot,[4] M. Timko,[17] P. Tipton,[10] S. Tkaczyk,[4] A. Tollestrup,[4] J. Tonnison,[13] W. Trischuk,[6] Y. Tsay,[3] F. Ukegawa,[18] D. Underwood,[1] S. Vejcik, III,[8] R. Vidal,[4] R. G. Wagner,[1] R. L. Wagner,[4] N. Wainer,[4] J. Walsh,[11] T. Watts,[16] R. Webb,[17] C. Wendt,[20] W. C. Wester, III,[10] T. Westhusing,[12] S. N. White,[15] A. B. Wicklund,[1] H. H. Williams,[11] B. L. Winer,[10] A. Yagil,[4] A. Yamashita,[18] K. Yasuoka,[18] G. P. Yeh,[4] J. Yoh,[4] M. Yokoyama,[18] J. C. Yun,[4] and F. Zetti[12]

(CDF Collaboration)

[1]*Argonne National Laboratory, Argonne, Illinois 60439*
[2]*Brandeis University, Waltham, Massachusetts 02254*
[3]*University of Chicago, Chicago, Illinois 60637*
[4]*Fermi National Accelerator Laboratory, Batavia, Illinois 60510*
[5]*Laboratori Nazionali di Frascati, Istituto Nazionale di Fisica Nucleare, Frascati, Italy*
[6]*Harvard University, Cambridge, Massachusetts 02138*
[7]*University of Illinois, Urbana, Illinois 61801*
[8]*The Johns Hopkins University, Baltimore, Maryland 21218*
[9]*National Laboratory for High Energy Physics (KEK), Tsukuba, Ibaraki 305, Japan*
[10]*Lawrence Berkeley Laboratory, Berkeley, California 94720*
[11]*University of Pennsylvania, Philadelphia, Pennsylvania 19104*
[12]*Istituto Nazionale di Fisica Nucleare, University and Scuola Normale Superiore of Pisa, I-56100 Pisa, Italy*
[13]*Purdue University, West Lafayette, Indiana 47907*
[14]*University of Rochester, Rochester, New York 14627*

[15]Rockefeller University, New York, New York 10021
[16]Rutgers University, Piscataway, New Jersey 08854
[17]Texas A&M University, College Station, Texas 77843
[18]University of Tsukuba, Tsukuba, Ibaraki 305, Japan
[19]Tufts University, Medford, Massachusetts 02155
[20]University of Wisconsin, Madison, Wisconsin 53706
(Received 14 February 1991)

Using the Collider Detector at Fermilab, the W-boson differential cross section $d\sigma/dP_T$ is measured using $W\to e\nu$ events in proton-antiproton collisions at $\sqrt{s}=1.8$ TeV. A next-to-leading-order theoretical calculation agrees well with the data. The cross section (σ) for $P_T>50$ GeV/c is measured to be $423\pm58(\text{stat})\pm108(\text{syst})$ pb.

PACS numbers: 13.85.Qk, 14.80.Er

Quantum chromodynamics (QCD) ascribes the transverse momentum of W bosons (P_T^W) produced in $p\bar{p}$ collisions to associated production of one or more gluons or quarks with the W. Comparisons of the measured P_T^W distribution to recent next-to-leading-order calculations[1] provide a test of these QCD calculations. Deviations from the prediction at large P_T^W could indicate new physics beyond the standard model. The center-of-mass energy ($\sqrt{s}=1.8$ TeV) available to the Collider Detector at Fermilab[2] (CDF) allows a measurement of the P_T^W spectrum at larger P_T^W than previous measurements[3] at the CERN $p\bar{p}$ collider ($\sqrt{s}=0.63$ TeV).

The W bosons which decay into an electron and a neutrino are used to measure $d\sigma/dP_T$. The electron is restricted to the central region[4] ($|\eta\equiv-\ln\tan\theta/2|<1.1$) where a vertex time projection chamber, a drift chamber (CTC) in a 1.4-T axial magnetic field, Pb(Fe)-scintillator calorimeters, and proportional wire chambers (CES) at the depth of electromagnetic shower maximum provide good electron identification. The neutrino produces an imbalance in the transverse energy ($E_T\equiv E\sin\theta$) deposition. The missing E_T ($\not{E}_T$) is defined by

$$\not{E}_T=-\sum_i E_T^i\hat{\mathbf{n}}_i\,, \tag{1}$$

i = calorimeter tower number with $|\eta|<3.6$,

where $\hat{\mathbf{n}}_i$ is a unit vector perpendicular to the beam axis and pointing at the ith calorimeter tower. A perfect detector would give $\not{E}_T=\mathbf{E}_T^\nu$. For each event, P_T^W is reconstructed from the electron momentum and the $\not{E}_T$.

Events must pass an electron trigger requiring (i) a cluster in the central electromagnetic (EM) calorimeter with $E_T>12$ GeV; (ii) a track in the CTC (Ref. 5) with $P_T>6$ GeV/c pointing toward the cluster; and (iii) the cluster's ratio of energy in the hadronic (Had) calorimeter to the energy in the EM calorimeter, Had/EM, less than 12.5%. The sample is further reduced by requiring that (i) the electron transverse energy $E_T^{\text{ele}}>20$ GeV; (ii) Had/EM $<0.055+0.00045E^{\text{ele}}$(GeV); (iii) the ratio of electron energy to track momentum be less than 1.5; (iv) the match between the CES shower position and the track position be within 1.5 cm in the ϕ direction and 3.0 cm in the z direction; (v) the electron be isolated, $(E_c-E_T^{\text{ele}})/E_T^{\text{ele}}<0.1$, where E_c is the total transverse energy inside a cone with radius $R=(\Delta\eta^2+\Delta\phi^2)^{1/2}=0.4$ centered on the cluster; and (vi) the lateral profiles of the calorimeter shower and the CES shower be consistent with the profiles of test beam electrons. Finally, the electron is required to fall in the fiducial volume away from calorimeter cracks, and the event vertex is required to be within 60 cm (2σ) of the nominal interaction point. These requirements leave 4442 events.[6] The final inclusive W sample (2496 events) is selected by requiring $|\not{E}_T|>20$ GeV and eliminating events consistent with a Z decay or photon conversion ($\gamma\to e^+e^-$).

The remaining backgrounds are summarized in Table I. The total background fraction is approximately constant with P_T^W. The amount of QCD background (jets and semileptonic decay of b,c quarks) is determined by studying the isolation of electrons in both a background sample and a signal sample with no isolation requirement. The number of QCD background events in the final sample is taken as the number of nonisolated electrons in the signal sample scaled by the ratio of isolated to nonisolated electrons in the background sample. This background's spectrum shape is then determined from a background-rich data sample. The size and shape of the background from $W\to\tau\nu(\tau\to e\nu\nu)$ and remaining $Z\to ee$ and $Z\to\tau\tau(\tau\to e\nu\nu)$ events are estimated using the ISAJET (Ref. 7) Monte Carlo program with detector simulation. The $W\to\tau\nu$ background, which has the same shape as the signal, is removed using a scale factor (Table II). Finally, the background from heavy-top-quark decay is assumed to be zero events with

TABLE I. Event sample summary. The $W\to\tau\nu$ background is removed by the normalization factor given in Table II.

	Number of events
Candidates	2496
Backgrounds:	
QCD	45 ± 24
$Z\to e^+e^-$	34 ± 15
$Z\to\tau\tau(\tau\to e)$	8 ± 4
$W\to\tau\nu(\tau\to e)$	85 ± 10
Heavy top	00^{+31}_{-0}

TABLE II. Normalization factors. Each factor enters the normalization as a divisor.

	Value
Electron identification efficiency	0.84 ± 0.03
Background: $W \rightarrow \tau \nu$	1.034 ± 0.004
W's misidentified as	
Conversions	0.965 ± 0.015
Z's	$0.999^{+0.001}_{-0.01}$
Event-vertex cut at 2σ	0.954 ± 0.005
Integrated luminosity (pb^{-1})	4.05 ± 0.28
Assumed branching fraction	$\frac{1}{9}$

an upper limit of 31 events, corresponding to the expected signal from a top quark with $m_{\rm top} = 90\ \mathrm{GeV}/c^2$.[8]

The cross section is normalized from the efficiencies (Table II), acceptance, and integrated luminosity. The electron identification efficiency is measured using a sample of W's selected solely with strict cuts on the $\not\!\!E_T$ and has negligible dependence on P_T^W. The electron trigger efficiency, studied using a $\not\!\!E_T$ trigger, is included in the electron identification efficiency. A Monte Carlo program predicts $0.1^{+1.0}_{-0.1}\%$ of the W's are removed by the Z veto. The fraction of W events lost by cuts to remove photon-conversion electrons is estimated by cutting on two tracks of the *same* charge instead of *opposite* charge. The kinematic and fiducial acceptance versus P_T^W is determined from a Monte Carlo program[9] (PAPAGENO) using MRS2 structure functions.[10] The acceptance is $\sim(32 \pm 2)\%$ for $P_T^W < 80\ \mathrm{GeV}/c$ and rises to $\sim(45 \pm 5)\%$ at $P_T^W = 170\ \mathrm{GeV}/c$. The systematic uncertainty on the acceptance is determined by varying the structure functions and the detector simulation of the $\not\!\!E_T$. The integrated luminosity is $4.05 \pm 0.28\ \mathrm{pb}^{-1}$.[6]

Cracks between detector components and nonlinear calorimeter response to low-energy particles make the observed $\not\!\!E_T$ an inaccurate measure of the neutrino $\mathbf{E}_T$. The corrected $\not\!\!E_T$ ($\mathbf{E}_T^{\nu}$) is calculated by dividing the observed calorimeter energy into three distinct classes: the electron cluster, other clustered energy ($E_T^{\rm clus} > 10$ GeV),[11] and nonclustered energy. The nonclustered energy vector ($\mathbf{E}_T^{\rm nc}$) is defined to incorporate the small amount of energy not included in the other classes. The corrected value of the $\not\!\!E_T$ is found by substituting the corrected values of the $\mathbf{E}_T^{\rm ele}$, $\mathbf{E}_T^{\rm clus}$, and $\mathbf{E}_T^{\rm nc}$ into the following expression:

$$\not\!\!E_T = -\left(\mathbf{E}_T^{\rm ele} + \sum \mathbf{E}_T^{\rm clus} + \mathbf{E}_T^{\rm nc}\right). \qquad (2)$$

Studies of test beam electrons and inclusive electrons provide small corrections to the electron energy.[12]

A Monte Carlo program is tuned to reproduce the jet fragmentation and nonclustered energy observed in the data. The calorimeter's response to single hadrons is determined from test-beam and E/P studies of low-energy particles. Using the Monte Carlo program to convolute the jet fragmentation with the calorimeter response, an $E_T^{\rm clus}$-dependent energy correction is determined for a central cluster ($0.15 < |\eta| < 0.9$).[13] The correction is extrapolated to the remaining detector using a relative response derived by balancing the E_T in two jet events. This relative response incorporates the low response for clusters incident on detector cracks. The cluster correction's systematic uncertainty is estimated by examining the corrected $\not\!\!E_T$ in events containing jets and an expected $|\not\!\!E_T| \sim 0$. Using the Monte Carlo program to compare the observed $\mathbf{E}_T^{\rm nc}$ with the total momentum of particles not included in the clusters or the electron yields a scale factor of 2.0 ± 0.2 for the $\mathbf{E}_T^{\rm nc}$ correction. The systematic uncertainty is determined from balancing the electron and recoil energies in Z events, as described below.

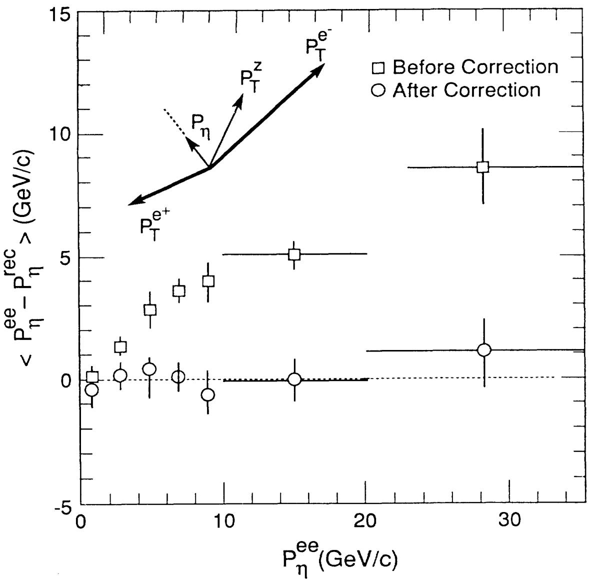

FIG. 1. The effect of the $\not\!\!E_T$ correction on Z events. The η direction is determined with the electrons but P_η can be determined with the electron momenta or the recoil energy. The difference, $P_\eta^{ee} - P_\eta^{\rm rec}$, is shown vs P_η^{ee}. Each error bar represents the uncertainty on the mean.

The $\not\!\!E_T$ corrections are verified with a $Z \rightarrow ee$ event sample. The component of P_T^Z that is parallel to the bisector of the electron directions ($\equiv P_\eta$) is well determined from the measured electron momenta. The component is also measured from the other calorimeter energy depositions (recoil energy). The recoil-energy measurement is subject to the same errors as the P_T^W measurement, and the same corrections can be applied. Figure 1 shows the mean difference between the electron measurement, P_η^{ee}, and the recoil-energy measurement, $P_\eta^{\rm rec}$, as a function of P_η^{ee}. After corrections, the difference is centered around 0.0 GeV/c for all P_η^{ee}. The lower region, $P_\eta^{ee} < 10$ GeV/c, is sensitive to the $\mathbf{E}_T^{\rm nc}$ scale factor, while the last two bins are sensitive to the cluster correction. A projection of the difference, fitted by a Gaussian distribution, gives a mean of 0.1 ± 0.3 GeV/c.

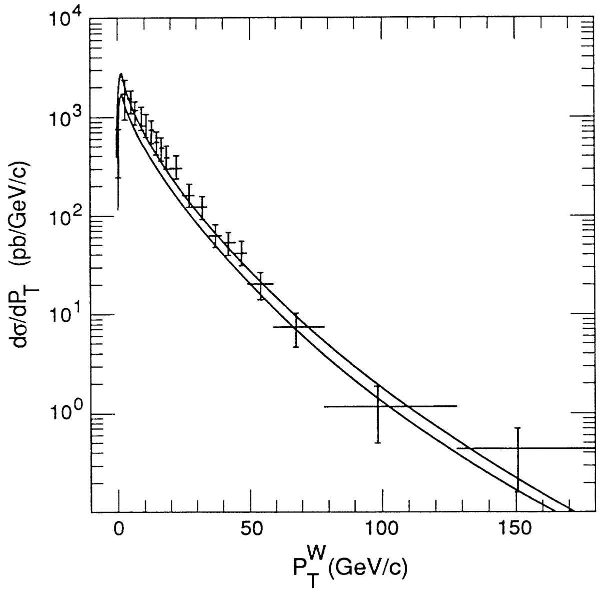

FIG. 2. The differential cross section $d\sigma/dP_T$ for W-boson production. The points are the measured values with combined systematic and statistical uncertainties. The band is a next-to-leading-order theoretical prediction (Ref. 1) with $\Lambda_{QCD} = 190$ MeV, $Q^2 = P_W^2$, and HMRS(B) structure functions [P. N. Harriman, A. D. Martin, W. J. Stirling, and R. G. Roberts, Phys. Rev. D **42**, 798 (1990)]. The horizontal error bars span the bin.

Detector resolution distorts the falling P_T^W distribution towards larger P_T^W. To correct for this effect, an empirical parametrization of the P_T^W spectrum is smeared using a resolution function determined from a detector simulation. The spectrum parameters are varied to find the best fit between the smeared spectrum and the data. The best fit is used to form a smearing correction which is the ratio between the parametrized spectrum before and after smearing. The correction is a scale factor between 1.9 and 0.83 for $P_T^W < 10$ GeV/c and between 0.87 and 0.97 for $P_T^W > 20$ GeV/c. The systematic uncertainty of the correction is determined by varying the resolution function and refitting.

The systematic uncertainties are propagated into the P_T^W spectrum by using a simple Monte Carlo program which varies each correction factor by its uncertainty. Each factor (luminosity, background, $\not{E}_T$ correction, etc.) is varied in a manner which preserves the correlations between the bins, thus providing a covariance matrix describing the correlations. The Monte Carlo program also incorporates the statistical uncertainty on the observed number of events.[13]

The fully corrected differential cross section $d\sigma/dP_T$ is shown in Fig. 2 and given in Table III. The error bars represent the combined statistical and systematic uncertainties. The integrated cross section for $P_T^W > 50$ GeV/c is 423 ± 58(stat) ± 108(syst) pb (2% of σ_{tot}). The theory predicts a cross section of 428 ± 64 pb.[1] The total integrated cross section is in agreement with our published value of σB.[6] In conclusion, the theoretical prediction is in good agreement with the measured W-boson transverse-momentum spectrum $d\sigma/dP_T$, and no significant deviations from the standard-model prediction are seen.

TABLE III. The cross section $d\sigma/dP_T$ vs P_T^W. The P_T^W values are corrected for binning effects.

P_T^W (GeV/c)	$d\sigma/dP_T \pm$ (stat) $\pm$ (syst) [pb/(GeV/c)]
1.0	694 $\pm 75 \pm 451$
3.0	1562 $\pm 102 \pm 677$
5.0	1419 $\pm 84 \pm 382$
7.0	1084 $\pm 68 \pm 219$
9.0	963 $\pm 61 \pm 196$
11.0	762 $\pm 54 \pm 173$
13.0	684 $\pm 51 \pm 164$
15.0	521 $\pm 45 \pm 122$
17.0	451 $\pm 43 \pm 104$
19.0	388 $\pm 40 \pm 86$
22.5	291 $\pm 22 \pm 65$
27.5	154 $\pm 16 \pm 33$
32.5	115 $\pm 14 \pm 24$
37.5	61.1 $\pm 9.9 \pm 12.8$
42.5	51.5 $\pm 9.2 \pm 10.6$
47.5	40.4 $\pm 8.1 \pm 8.3$
54.7	19.6 $\pm 4.0 \pm 4.4$
68.9	7.3 $\pm 1.7 \pm 2.1$
99.6	1.18 $\pm 0.41 \pm 0.55$
151.2	0.44 $\pm 0.24 \pm 0.15$

We thank the Fermilab Accelerator Division and the CDF support staff for an excellent job. We would also like to thank Peter Arnold, Russel Kauffman, and Kevin Einsweiler for useful discussions. This work was supported by the DOE, the NSF, the Istituto Nationale di Fisica Nucleare, the Ministry of Science, Culture and Education of Japan, and the A. P. Sloan Foundation.

[a]Visitor.

[1]P. Arnold and M. H. Reno, Nucl. Phys. **B319**, 37 (1989); **B330**, 284(E) (1990); P. B. Arnold and R. P. Kauffman, Phys. Lett. B **349**, 381 (1991).

[2]F. Abe *et al.*, Nucl. Instrum. Methods Phys. Res., Sect. A **271**, 387 (1988).

[3]UA2 Collaboration, J. Alitti *et al.*, Z. Phys. C **47**, 523 (1990); UA1 Collaboration, C. Albajar *et al.*, Z. Phys. C **44**, 15 (1989).

[4]The CDF coordinate system defines z along the proton beam direction, θ as the polar angle, and ϕ as the azimuthal angle.

[5]G. W. Foster *et al.*, Nucl. Instrum. Methods Phys. Res., Sect. A **269**, 93 (1988).

[6]For more on electron selection and luminosity measurement, see F. Abe *et al.*, Phys. Rev. D (to be published).

[7]F. Paige and S. D. Protopopescu, BNL Report No. 38034,

1986 (unpublished). ISAJET version 6.25 was used.

[8]The current mass limit of the top quark is 89 GeV/c^2. K. Sliwa, in *Proceedings of Twenty-Fifth Recontres de Moriond, Les Arcs, Savoie, France, 1990* (Edition Frontieres, Gif-sur-Yvette, 1990), p. 456, M65.

[9]I. Hinchliffe (to be published). PAPAGENO version 3.12 was used.

[10]A. D. Martin, R. G. Roberts, and W. J. Stirling, Phys. Rev. D **37**, 1161 (1988).

[11]A cluster cone size of $R=(\Delta\eta^2+\Delta\phi^2)^{1/2}=0.7$ was used. For a description of clustering technique, see F. Abe *et al.*, Phys. Rev. Lett. **62**, 613 (1989).

[12]F. Abe *et al.*, Phys. Rev. D **43**, 2070 (1991).

[13]Brian L. Winer, Ph.D. thesis, University of California, Berkeley, 1991. The complete covariance matrix can be found in this reference.